# BMP signaling is required for the generation of primordial germ cells in an insect

Seth Donoughe[a], Taro Nakamura[a], Ben Ewen-Campen[a], Delbert A. Green II[b], Lory Henderson[b], and Cassandra G. Extavour[a,1]

Departments of [a]Organismic and Evolutionary Biology and [b]Molecular and Cellular Biology, Harvard University, Cambridge, MA 02138

Edited by Anthony P. Mahowald, The University of Chicago, Chicago, IL, and approved February 7, 2014 (received for review January 10, 2014)

**Two modes of germ cell formation are known in animals. Specification through maternally inherited germ plasm occurs in many well-characterized model organisms, but most animals lack germ plasm by morphological and functional criteria. The only known alternative mechanism is induction, experimentally described only in mice, which specify germ cells through bone morphogenetic protein (BMP) signal-mediated induction of a subpopulation of mesodermal cells. Until this report, no experimental evidence of an inductive germ cell signal for specification has been available outside of vertebrates. Here we provide functional genetic experimental evidence consistent with a role for BMP signaling in germ cell formation in a basally branching insect. We show that primordial germ cells of the cricket *Gryllus bimaculatus* transduce BMP signals and require BMP pathway activity for their formation. Moreover, increased BMP activity leads to ectopic and supernumerary germ cells. Given the commonality of BMP signaling in mouse and cricket germ cell induction, we suggest that BMP-based germ cell formation may be a shared ancestral mechanism in animals.**

TGF-β | inductive signaling | Orthoptera | germ line | *piwi*

There are two well-characterized modes of animal germ cell specification. In the inheritance mode, observed in *Drosophila melanogaster*, *Caenorhabditis elegans*, and *Xenopus laevis*, maternally provided cytoplasmic determinants (germ plasm) specify a subset of early embryonic cells as germ cells. In contrast, mice specify their germ line through the induction mode, in which a zygotic cell–cell signaling mechanism specifies germ cells later in development. We previously hypothesized that the inductive mode was ancestral among metazoans and that the inheritance mode had evolved independently in multiple derived lineages (1, 2). Consistent with this hypothesis, multiple basally branching insects do not segregate maternally provided germ plasm, unlike the relatively derived *Drosophila* model (3, 4). However, experimental evidence for the inductive mode was available only for salamanders (5, 6) and mice (7–10), and to date, inferences of induction outside of vertebrates have been based on gene expression and cytological data (1, 11–16).

Because *Drosophila* is highly derived with respect to many aspects of development (17), we examined germ cell development in the cricket *Gryllus bimaculatus*, a basally branching insect that may shed light on putative ancestral mechanisms of specifying germ cells. We previously showed that unlike *Drosophila*, *Gryllus* primordial germ cell (PGC) specification requires zygotic mechanisms rather than germ plasm or the *oskar* germ-line determinant (4, 18). However, the signals that might induce PGC formation in *Gryllus* remained unknown. Because mammals require the highly conserved bone morphogenetic protein (BMP) pathway to specify PGCs (8–10, 19, 20), we investigated BMP signaling as a candidate for regulating inductive germ cell specification in *Gryllus*.

## Results and Discussion

*Gryllus* PGCs first arise among the abdominal mesoderm 2.5 d after egg laying (AEL) (4). To determine whether *Gryllus* PGCs actively transduce BMP signals during their formation, we used multiplex immunostaining to simultaneously detect the PGC marker *Gryllus bimaculatus piwi* orthologue (Gb-Piwi) (4) and the BMP signal effector phosphorylated Mad (pMad) (20). We observed coexpression of high levels of Gb-Piwi and nuclear pMad in mesodermal cells of anterior abdominal segments, revealing that there is active BMP signaling in PGCs at the time that they are specified, and in most PGCs while they coalesce into clusters (Fig. 1 *A–C'''*). We also detected nuclear pMad in both ectodermal and mesodermal cells. This somatic expression was detected at the highest levels laterally (dorsally) and decreased toward the medial (ventral) region, becoming undetectable at 7–10 cell diameters from the lateral (dorsal) edge of the embryo along the entire anterior–posterior axis (Fig. 1 *A–C* and *SI Appendix*, Fig. S2 *A–A'''*). This graded expression pattern is consistent with a conserved role for BMP signaling in dorsoventral patterning (21). The expression of nuclear pMad in PGCs during their formation is also consistent with a role for BMP signaling in PGC specification.

Next, we examined the expression of multiple BMP pathway members in *Gryllus* embryos during PGC formation. *Gryllus* orthologs of vertebrate ligands *BMP2/4* (*Gryllus bimaculatus decapentaplegic*, *Gb-dpp1* and *Gb-dpp2*) and *BMP5/7/8* (*Gryllus bimaculatus glass bottom boat*, *Gb-gbb*) are expressed in the abdomen throughout the period of PGC formation, and are enriched at the dorsolateral margins of the embryo by 4 d AEL (Fig. 1 *D–F'* and *SI Appendix*, Figs. S1 and S2 *D–F'''*). Double labeling of BMP ligand expression and Gb-Piwi (4) confirmed that the BMP ligands *Gb-dpp1* and *Gb-dpp2* are expressed within 2–4 cell diameters of the PGCs (Fig. 1 *D'''–E'''*), and *Gb-gbb* is expressed in cells adjacent to the PGCs (Fig. 1*F'''*). BMP receptors *Gryllus bimaculatus thickveins*

### Significance

**Many model organisms specify germ cells using maternally supplied germ-line determinants. In contrast, mice rely on embryonic cell–cell signaling to induce cells to become germ cells. Molecular evidence for inductive germ-line specification had previously been provided only for the mouse. Here we provide functional evidence for inductive germ cell specification in an invertebrate, by showing that bone morphogenetic protein (BMP) signaling, which induces mouse germ cell specification, is required for establishment of embryonic germ cells in a cricket. BMP pathway knockdown causes reduction or loss of germ cells, and elevated levels of BMP signaling cause supernumerary and ectopic germ cells. BMP-based germ cell induction in mice and crickets suggests that this may be a shared ancestral mechanism in animals.**

Author contributions: S.D., T.N., and C.G.E. designed research; S.D., T.N., B.E.-C., D.A.G., L.H., and C.G.E. performed research; S.D., T.N., B.E.-C., and C.G.E. analyzed data; and S.D. and C.G.E. wrote the paper.

The authors declare no conflict of interest.

This article is a PNAS Direct Submission.

Data deposition: The sequences reported in this paper have been deposited in the GenBank database (accession nos. KF670859–KF670865).

[1]To whom correspondence should be addressed. E-mail: extavour@oeb.harvard.edu.

This article contains supporting information online at www.pnas.org/lookup/suppl/doi:10.1073/pnas.1400525111/-/DCSupplemental.

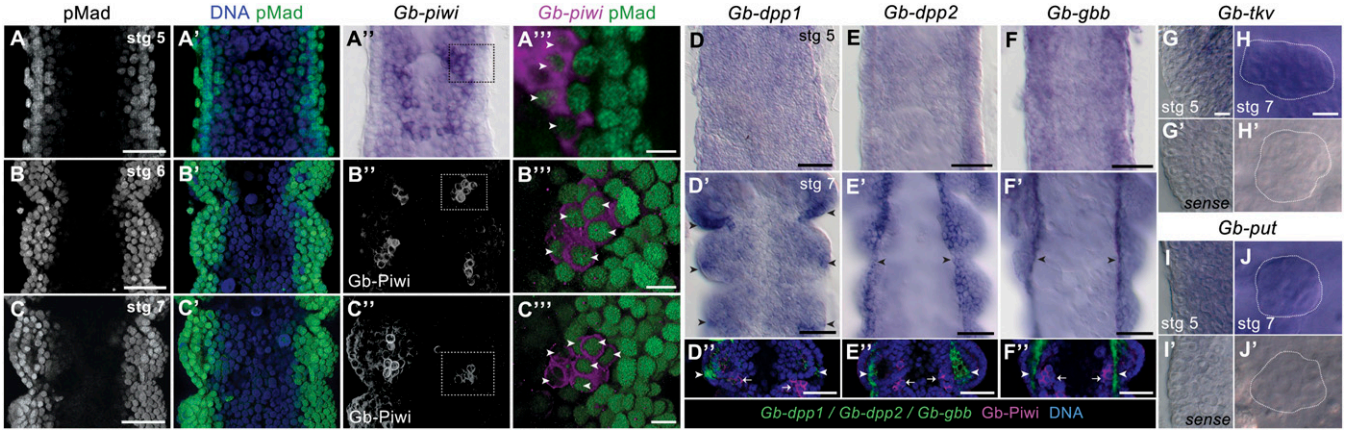


**Fig. 1.** Expression of BMP pathway components during *Gryllus* PGC formation. (*A–C‴*) Embryos triple stained for nuclei (Hoescht 33342), pMad, and Gb-Piwi at developmental stages 5 through 7, when PGCs are first forming, show that PGCs contain nuclear pMad. Micrographs show single optical sections parallel to the anterior–posterior axis through the dorsal region of anterior abdominal segments, showing the mesoderm flanked by a single layer of ectodermal cells at both lateral margins of the embryo. (*A–C*) Nuclear pMad signal is highest in lateral (dorsal) ectodermal and mesodermal cells and absent from medial (ventral) mesodermal cells. Costaining with *Gb-Piwi* transcripts (*A*) or Gb-Piwi protein (*B* and *C*) reveals nuclear pMad in PGCs. Boxed regions in *A″–C″* are magnified and shown in volume projections in *B‴* and *C‴*. Arrowheads indicate pMad-positive PGCs. As previously documented (4), Gb-Piwi is detectable at the highest levels in PGCs but is also present at lower levels in some mesodermal and ectodermal cells at these stages. (*D–F″*) BMP ligand expression. In stage 5 embryos, *Gb-dpp1* (*D*), *Gb-dpp2* (*E*), and *Gb-gbb* (*F*) are not enriched along the dorsal edge, in contrast to pMad staining (*A*). In stage 7 embryos, *Gb-dpp1* is expressed in ectodermal foci in each segment, and *Gb-dpp2* and *Gb-gbb* are expressed along the dorsal edge of the embryo. Abdominal segments A1–A3 are shown; arrowheads indicate strong ligand expression. (*D″-F″*) Embryos double-stained for BMP ligands (green, indicated by arrowheads) and Piwi protein (magenta, single optical section, indicated by arrows). (*G–J*) Receptors *Gb-tkv* and *Gb-put* are expressed ubiquitously throughout embryogenesis, including in PGCs. (*G*, *G′*, *I*, and *I′*) A dorsal focal plane of stage 5 embryos, where PGCs form. White outlines in *H*, *H′*, *J*, and *J′* indicate PGC clusters in stage 7 embryos. Anterior is up; A2 is the anteriormost segment shown in each panel. [Scale bar, 10 μm in *A‴*, *B‴*, *C‴*, *G*, and *H* (also applies to *G′–J′*), and 50 μm in all other panels.]

*(Gb-tkv)* (type I) and *Gryllus bimaculatus punt (Gb-put)* (type II) and the BMP effector Smad1/5/8 (*Gryllus bimaculatus Mothers against dpp, Gb-Mad*) are expressed ubiquitously, including in PGCs, throughout PGC specification and cluster coalescence (Fig. 1 *G–J′* and *SI Appendix*, Fig. S2 *B–C″* and *G–J″*). In summary, these expression data indicate that PGCs are competent to receive BMP signals, that BMP ligands are expressed in neighboring and nearby cells and thus could serve as a source of inductive signals, and that PGCs are responding to BMP signals at the time of their specification and throughout subsequent PGC cluster coalescence.

To test for a requirement for BMP signaling in PGC specification, we used RNA interference [RNAi, validated with quantitative PCR (qPCR) and quantification of pMad levels; *SI Appendix*, Fig. S3] to knock down each BMP ligand and the effector *Gb-Mad*. Many BMP pathway RNAi embryos displayed severe morphological defects suggestive of dorsalization, consistent with a conserved role for BMP signaling in dorsoventral patterning (21). However, we also obtained less severely affected RNAi embryos that developed to 4 d AEL, showed normal axial patterning, and possessed all body segments. Despite their generally normal appearance, these embryos displayed reduced pMad levels in the region where PGCs arise (Fig. 2 *L–P* and *SI Appendix*, Fig. S3 *E–L*) and abnormalities in leg development, confirming that BMP signaling was compromised. We quantified PGC defects in these embryos (*SI Appendix*, Figs. S4–S6) and found that 50% of *Gb-Mad* RNAi embryos lacked PGCs ($P < 0.05$, $n = 18$; Fig. 2*C* and *SI Appendix*, Table S3), which was never observed in control embryos ($n = 40$), and the remaining 50% of *Gb-Mad* RNAi embryos had significantly smaller PGC clusters ($P < 0.001$, $n = 180$; Fig. 2*H*) and significantly fewer PGCs than controls ($P < 0.001$, $n = 18$; Fig. 2*A*). Knockdown of BMP ligands also reduced or abolished PGCs, with *Gb-gbb* RNAi embryos showing the most severe phenotype. A total of 30.2% of *Gb-gbb* RNAi embryos lacked PGCs altogether ($P < 0.001$, $n = 43$; *SI Appendix*, Table S3), and the remaining 69.8% of embryos showed significant reduction of PGC cluster size ($P < 0.001$, $n = 430$; Fig. 2 *F* and *K*) and total PGC number per embryo ($P < 0.001$, $n = 43$; Fig. 2*A*). *Gb-dpp1* RNAi resulted in total PGC loss in 12.5% of embryos ($n = 32$; *SI Appendix*, Table S3), and significantly reduced PGC cluster size ($P < 0.001$, $n = 401$; Fig. 2 *D* and *I*) and total PGC number ($P < 0.05$, $n = 32$; Fig. 2*A*) in the remainder. *Gb-dpp2* RNAi embryos did not show a significant decrease in PGC number ($P = 0.67$, $n = 18$; Fig. 2*A*). Consistent with the observation that *Gb-gbb* is expressed in cells closer to the emerging PGCs than either *Gb-dpp* ortholog (Fig. 1*F″*), this suggests that *Gb-gbb* signals may be more important for PGC formation than *Gb-dpp* signals. However, we note that *dpp* signals have been shown to operate across distances of up to 10–15 cell diameters in other organisms (22), consistent with our RNAi data showing that *Gb-dpp1* also contributes to PGC formation, albeit more modestly than *Gb-gbb*. We noted that not all segments of a given embryo were equally severely affected with respect to PGC number: A3 was least affected by *Gb-dpp1* and *Gb-dpp2* RNAi (Fig. 2 *I* and *J*), whereas A2 and A4 appeared marginally less affected than other segments in *Gb-Mad* and *Gb-gbb* RNAi embryos, respectively (Fig. 2 *H* and *K*). These results indicate a requirement for BMP signaling in *Gryllus* PGC development, with *Gb-gbb* likely being the most relevant BMP ligand.

Given that mesoderm is required for *Gryllus* PGC specification (4) and that BMP signaling is required for mesoderm development in many animals (23–27), we considered the possibility that BMP pathway knockdown was disrupting PGC specification indirectly through mesodermal absence or death. At 2.5 d AEL, *Gryllus* mesodermal cells can be unambiguously identified by cellular morphology and anatomical position (28, 29) (*SI Appendix*). We found that in BMP pathway RNAi experiments, embryos at the PGC specification stage (2.5 d AEL) had formed mesoderm correctly (*SI Appendix*, Fig. S7 *A–J′*). Moreover, there was no increase in the number of apoptotic mesodermal cells (*SI Appendix*, Fig. S7*K*). Thus, the loss of PGCs in BMP RNAi treatments is unlikely to be due to a failure of mesoderm specification or death of mesoderm or PGCs. Because it is difficult to quantify *Gryllus* PGCs before PGC cluster formation, we cannot compare PGC proliferation rates directly between RNAi and control embryos.

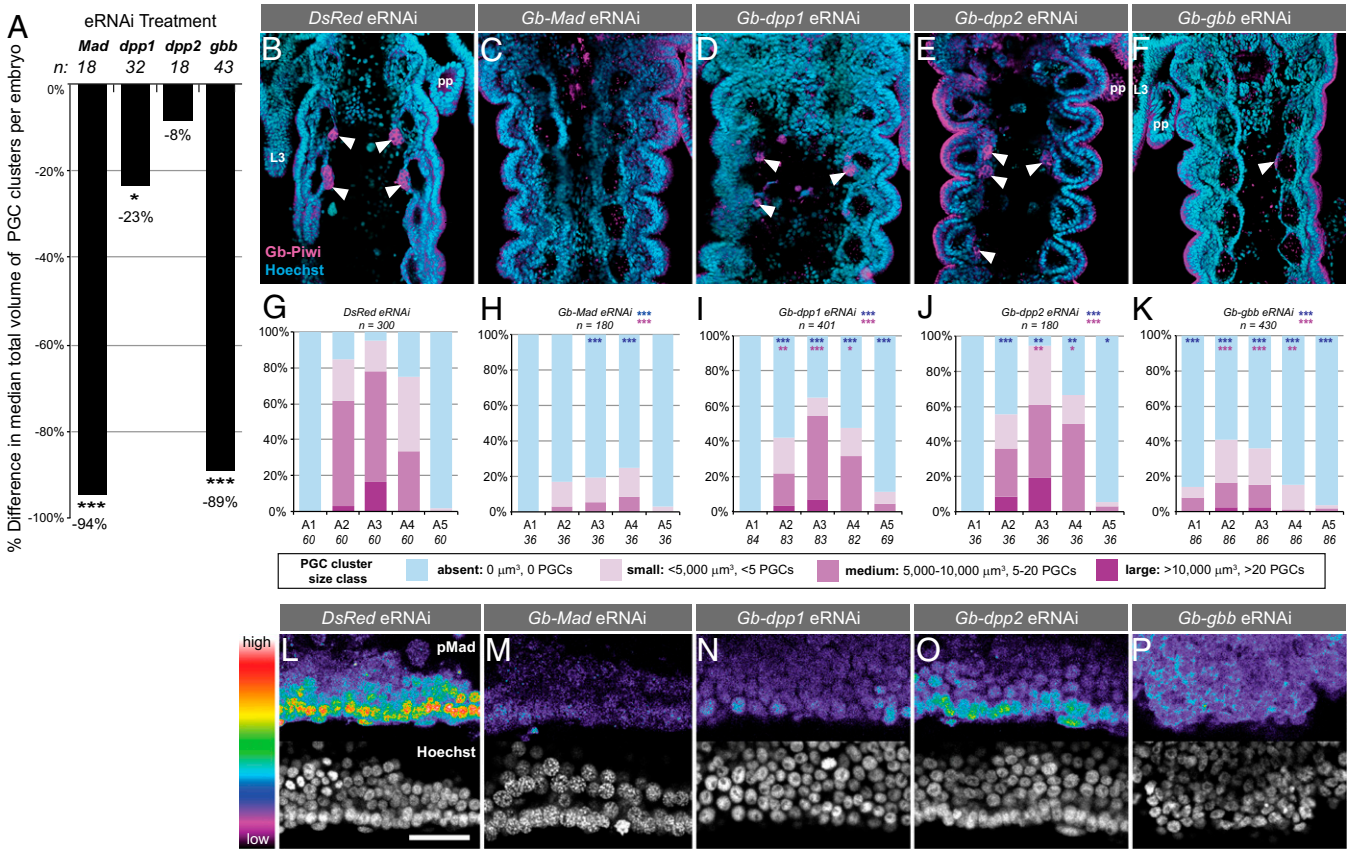


**Fig. 2.** BMP signaling is required for *Gryllus* PGC specification. RNAi against *Gryllus* BMP pathway members results in loss or reduction of PGCs. (*A*) Percent difference between the median total volume of PGCs clusters per embryo in each knockdown condition compared with controls. (*B–F*) Abdominal segments A1–A5 in a representative embryo from each RNAi treatment at 4 d AEL. PGCs (arrowheads) identified with anti–Gb-Piwi (magenta); anterior is up. (Scale bar, 50 μm.) As previously reported (4), Gb-Piwi expression is also detectable in ectodermal cells at this stage of development. (*G–K*) PGC quantification per segment at 4 d AEL for each BMP pathway RNAi treatment. Blue asterisks indicate significance of presence/absence of PGC clusters compared with controls; pink asterisks indicate significance of size differences of PGC clusters compared with controls. (*L–P*) pMad expression shown with rainbow heat map (white/red, highest levels; purple/black, lowest levels) in the lateral A3 mesoderm at 2.5 d AEL, where PGCs arise, in representative RNAi embryos. Anterior is left. (Scale bar, 50 μm.) Mann–Whitney test significance in *A* and *G–K*, $*P < 0.05$, $**P < 0.01$, $***P < 0.001$.

However, the complete absence of PGCs in a significant proportion of *Gb-Mad* and *Gb-gbb* RNAi embryos and the absence of apoptotic PGCs in all RNAi experiments suggest a direct requirement for BMP signaling in *Gryllus* PGC specification.

We hypothesized that if BMP signaling acts as a direct inductive signal in PGC specification, then elevated or ectopic levels of BMP signaling might increase the number of PGCs formed or cause them to form in ectopic locations. To test this hypothesis, we took two approaches to raise BMP signaling activity in early embryos above wild-type levels: (*i*) injecting 4′-hydroxychalcone, a recently identified chemical activator of the BMP pathway (30), and (*ii*) injecting recombinant *D. melanogaster* Decapentaplegic (Dpp) protein (Dm-Dpp) (*SI Appendix*, Figs. S8 and S9). In both treatments, axial patterning, mesoderm formation, and overall embryonic morphology appeared normal in experimental embryos, but nuclear pMad levels at the time of PGC specification were slightly elevated and expanded toward the ventral midline with respect to controls (Fig. 3 *M–O* and *SI Appendix*, Fig. S10 *A–D*). PGC cluster size showed a dose-dependent increase in every segment of treated embryos (Fig. 3 *D–F′* and *SI Appendix*, Fig. S10*E*). Summing the volumes of all PGC clusters in an embryo showed that the total number of PGCs per embryo was increased by up to 42% (Fig. 3*G*), consistent with activation of BMP signaling. In addition, both treatments caused a significantly increased frequency of ectopic PGCs, defined as PGCs found in segments A1, A5, or A6 (10 mM 4′-hydroxychalcone, $P < 0.01$, $n = 31$, Fig. 3 *E′* and *L*; 10 μg/mL Dm-Dpp, $P < 0.01$, $n = 23$, Fig. 3 *F* and *J–L*; 100 μg/mL Dm-Dpp, $P < 0.05$, $n = 15$, Fig. 3 *F′* and *L*). Ectopic and supernumerary PGCs were not randomly distributed, but instead were clustered adjacent to the coelomic pouches like wild-type PGCs (Fig. 3 *C*, *C′*, *I*, and *K*). Ectopic PGCs are unlikely to result from mismigration, as *Gryllus* PGCs arise in the segments that will house the gonad primordium (A2–A4) and, unlike PGCs in *Drosophila* or mice, do not undergo long-range migration (4). To definitively eliminate the possibility of BMP-induced mismigration, one would need to track PGCs in vivo, a technique that is not currently possible in *Gryllus*.

Some embryos treated with Dm-Dpp displayed an increase in the proportion of A2–A4 segments lacking PGCs (*SI Appendix*, Fig. S10 *F* and *H*). We note, however, that a low level of PGC loss in these segments can be a nonspecific consequence of embryo perturbation, even in buffer-only injected controls, and that the proportion of these segments lacking PGCs in 4′-hydroxychalcone–treated embryos was not significantly different from controls (*SI Appendix*, Fig. S10 *F–H*). We think it unlikely that BMP signaling actively represses PGC formation, as this hypothesis does not explain the supernumerary or ectopic PGCs induced by the BMP activation treatments. However, the altered distribution of PGCs induced by widespread BMP activation suggests that PGC specification is not solely dependent on BMP levels, but instead may involve a range of acceptable BMP signal levels integrated with

DEVELOPMENTAL BIOLOGY

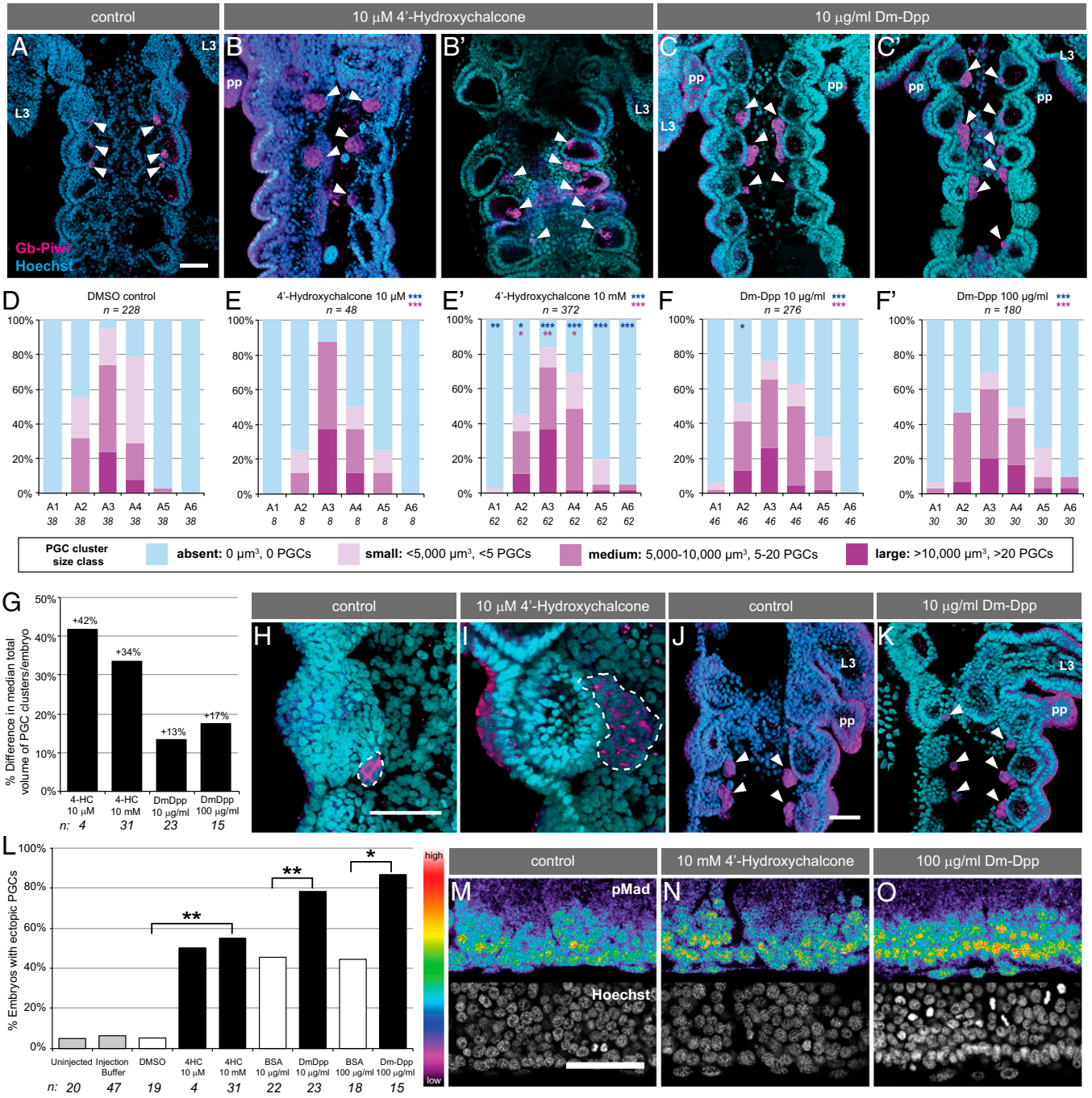


**Fig. 3.** Elevated BMP signaling levels induce supernumerary and ectopic *Gryllus* PGCs. Abdominal segments A1–A6 from (*A*) a representative DMSO control embryo (BSA controls were similar), (*B* and *B′*) 10 μM 4′-hydroxychalcone–injected, and (*C* and *C′*) 10 μg/mL Dm-Dpp–injected embryos at 4 d AEL. PGCs (arrowheads) identified with anti–Gb-Piwi (magenta); anterior is up. (Scale bar, 50 μm.) L3, third thoracic leg; pp, pleuropodia. A1 is the anterior-most segment in each panel unless otherwise indicated. (*D*–*F′*) Quantification of total PGCs per segment at 4 d AEL in control and experimental embryos. Asterisks indicate significance as described in the Fig. 2 legend. (*G*) Percent difference between median total volume of PGC clusters per embryo in each knockdown condition compared with controls. (*H* and *I*) Higher magnification views of a single PGC cluster (white outline) in a control (DMSO) and a 10 μM 4′-hydroxychalcone–injected embryo. Gb-Piwi expression appears patchy in PGCs because it is localized to the cytoplasm and PGCs have a high nuclear:cytoplasmic ratio (4). (*J* and *K*) Higher magnification views of PGC clusters in a control (10 μg/mL BSA) and 10 μg/mL Dm-Dpp–injected embryos. PGCs are present only in segments A2 and A3 in controls (*J*), but are present ectopically in segment A1 in Dm-Dpp–injected embryos (*K*). (*L*) Quantification of ectopic PGC clusters in BMP-activated embryos compared with controls. Bars represent percent of embryos in each treatment that have at least one ectopic PGC cluster. (*M*–*O*) pMad expression shown with rainbow heat map (white/red, highest levels; purple/black, lowest levels) in the lateral A3 mesoderm at 2.5 d AEL, where PGCs arise, in representative control and BMP-activated embryos. Anterior is left; dorsal margin is down. (Scale bar, 50 μm.) Mann–Whitney test significance in *D*, *E*, *E′*, *F*, *F′*, and *G*–*L*, $*P < 0.05$, $**P < 0.01$, $***P < 0.001$.

additional segment-specific positional information. This hypothesis is additionally consistent with the expression of nuclear pMad during PGC formation (Fig. 1 *A*–*C* and *SI Appendix*, Fig. S2 *A*–*A″*), as the presence of nuclear pMad in some non-PGC cell types suggests that additional mechanisms may be involved in PGC specification. In mice, where BMP signaling induces PGC formation,

phosphorylated SMAD is also detectable in multiple somatic cells, including cells neighboring the nascent PGCs (31). A combination of antagonistic and competence signals operate together with BMP signaling to ensure mouse PGC specification in only a subset of phosphorylated SMAD-positive cells, and we hypothesize that analogous mechanisms may be operative in *Gryllus*. Thus, although we cannot formally rule out additional roles for BMP signaling in migration, maintenance, and/or proliferation of PGCs, we propose that our results are most consistent with the hypothesis that BMP signaling induces PGC specification in *Gryllus*.

We have provided evidence that cricket PGCs are specified via BMP signaling, which appears to be necessary for cricket PGC formation. These data represent, to our knowledge, the first functional genetic evidence for an inductive mode of invertebrate germ cell specification. Our results support a model whereby *Gb-gbb* signals (and to a lesser extent *Gb-dpp1* signals) from the dorsolateral abdominal ectoderm are transduced via *Gb-Mad* in the adjacent mesoderm and cause some of those cells to adopt PGC fate. The presence of supernumerary germ cells in BMP activation experiments and the reduction in PGC cluster size in RNAi experiments raise the possibility that BMP signaling promotes PGC proliferation as well as, or rather than, specification. However, this hypothesis does not account for the presence of ectopic PGCs, given that *Gryllus* PGCs do not undertake long-term migration (4), nor for the complete absence of PGCs in *Gb-gbb* and *Gb-Mad* RNAi experiments, given that PGC clusters are derived from a large number of initially specified precursors rather than just one or a few cells (4).

The fact that ectopic germ cells are found only in lateral positions may be because although pMad levels are elevated by both treatments (Fig. 3 *M–O*), the shape of the activation profile is the same as that of wild-type embryos: nuclear pMad is at the highest levels dorsolaterally, where PGCS are specified, and at the lowest levels ventrally, where PGCs are never observed (*SI Appendix*, Fig. S10 *B* and *D*). We hypothesize that an inhibitory ventral signal, possibly of the *sog*/*Chordin* family, may restrict BMP signaling to dorsal tissues. Alternatively or in addition, a lateral competence signal may play a role in ensuring that not all cells expressing high levels of nuclear pMad differentiate as PGCs. With respect to their specification at the correct position along the anterior–posterior axis, the mechanism(s) that restricts PGC formation to the lateral mesoderm of segments A2–A4 in wild-type embryos are currently unknown. The appearance of ectopic PGCs anterior and posterior to wild-type positions in BMP activation experiments suggests that sufficiently high BMP signaling activity may perturb or overcome the positional information, potentially *Hox* gene-mediated, that normally limits PGC specification along the anterior–posterior axis. Our observation of segment-specific effects on PGC number in both the RNAi and BMP activation experiments is consistent with this model, as it suggests that PGC sensitivity to BMP signaling varies along the anterior–posterior axis.

Our findings in the cricket are similar to those observed in mouse PGC specification. In both cases, an ectodermal BMP signal induces a competent subset of mesoderm to become PGCs (32). PGC phenotypes are observable only in mildly knocked down *Gryllus* embryos, or in heterozygous knockout mice (8–10), as strong RNAi phenotypes and homozygous knockout conditions severely disrupt early development. Loss of BMP2/4, BMP8, and SMAD1/5/8 orthologs leads to loss or reduction of PGCs in both systems (Fig. 4*A*). Two parsimonious evolutionary scenarios based on functional genetic data that could explain the mechanistic similarities observed in cricket and mouse PGC specification are that BMP-based PGC induction (*i*) originated in a Bilaterian ancestor (denoted by a red diamond in Fig. 4*B*) or (*ii*) evolved independently within amniotes and insects (red text in Fig. 4*B*). Given that, to our knowledge, a role for BMP signaling in PGC formation has been directly tested in only two phyla, at present it is difficult to determine which of these hypotheses is more likely. However, in support of the first hypothesis, we note that in multiple metazoan phyla, germ cells are responsive to BMP signaling at some stage of their development, including PGC specification, gametogenesis, germ-line stem cell divisions, and adoption of germ cell fate by stem cells in culture (Fig. 4*B* and *SI Appendix*). This suggests that in addition to its conserved role in dorsoventral patterning (21), there is an ancient and widespread association of BMP signaling with germ cell fate or pluripotency. If future studies reveal a role for BMP signaling in PGC formation in additional taxa that use the inductive mode, that

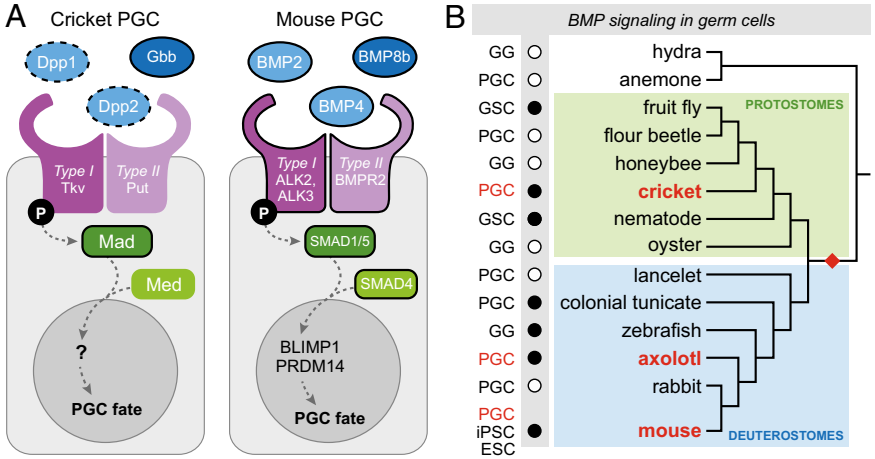


**Fig. 4.** BMP signaling in germ cells across the Metazoa. (*A*) Hypothetical model for BMP pathway function in cricket and mouse PGCs. Homologous proteins are shown in the same color. Black outlines indicate molecules whose role in germ cells has been tested experimentally through knockdown or knockout experiments; dotted black outline of Gb-Dpp orthologs indicates a potentially minimal or absent requirement in PGC specification. Ligand–receptor interactions are schematized only, as the specific interactions are unknown for both systems. (*B*) Phylogenetic distribution of animals for which expression (white circles) or functional (black circles) data suggest that BMP signaling is involved in some aspect of germ cell development (*SI Appendix*): ESC, conversion of embryonic stem cells to germ cells; GG, gametogenesis; GSCs, germ-line stem cells; iPSC, conversion of induced pluripotent stem cells to germ cells; PGCs, primordial germ cells. Red text indicates animals for which functional data support a role for BMP signaling in PCG specification; these data could support a hypothesis of convergent evolution of BMP-based germ cell formation in two or more bilaterian clades. Red diamond indicates the hypothesis of an ancestral role for BMP signaling in bilaterian PGC formation.

would further support the hypothesis that BMP signaling constitutes an ancestral animal mechanism for specification of the germ line.

## Materials and Methods

Genes were cloned using sequences from the *Gryllus* developmental transcriptome (33), with additional sequence data kindly provided by T. Mito (University of Tokushima, Japan). All sequences reported in this study have been deposited in GenBank under accession nos. KF670859–KF670865. *Gryllus* culturing, phylogenetic analysis, in situ hybridization, immunostaining, dsRNA synthesis, and qPCR were conducted as previously described (4). Zygotic RNAi was achieved by injection of dsRNA at either 0–5 h AEL or 24–36 h AEL using previously described injection techniques (4). Small molecule activation of the BMP pathway was accomplished by injecting eggs at 0–5 h AEL with (*i*) either 10 μM or 10 mM of 4′-hydroxychalcone (30) (Santa Cruz Biotechnology Chemicals SC-262260) in DMSO, with DMSO as a control, and (*ii*) either 10 μg/mL or 100 μg/mL of recombinant Dm-Dpp protein (R&D Systems 159-DP-020/CF) in dilute HCl as per the manufacturer's instructions, with 10 or 100 μg/mL of BSA in dilute HCl as a control. To quantify PGCs, the volume of each PGC cluster at 4 d AEL was calculated as an ellipsoid with confocal micrographs of optical sections through the region of the abdomen containing germ cells (*SI Appendix*, Fig. S4). The volume of each PGC in a cluster was both independent of the number of PGCs in a cluster and unaffected by BMP RNAi treatments. The calculated volume of a whole PGC cluster was thus strongly positively correlated with the number of PGCs in that cluster. Measurements of PGC cluster volume, which were more efficient than directly counting PGCs, therefore allowed us to accurately determine the total number of PGCs per cluster, per segment, and per embryo.

**ACKNOWLEDGMENTS.** We thank T. Mito for the *Gb-dpp2* sequence; D. Vasiliauskas, S. Morton, T. Jessell, E. Laufer, and S. Kunes for reagents; A. Ahuja for discussion of statistical analysis; and W. Gelbart, M.H.T. Extavour, and Extavour lab members for discussion. This research was supported by National Science Foundation (NSF) Grants IOS-1257554 and IOS-1257217 (to C.G.E.), a Ford Foundation Dissertation Fellowship (to D.A.G.), and NSF Graduate Training Fellowships (to S.D., D.A.G., and B.E.-C.).

1. Extavour CG, Akam ME (2003) Mechanisms of germ cell specification across the metazoans: Epigenesis and preformation. *Development* 130(24):5869–5884.
2. Extavour CG (2007) Evolution of the bilaterian germ line: Lineage origin and modulation of specification mechanisms. *Integr Comp Biol* 47(5):770–785.
3. Ewen-Campen B, Jones TE, Extavour CG (2013) Evidence against a germ plasm in the milkweed bug *Oncopeltus fasciatus*, a hemimetabolous insect. *Biol Open* 2(6): 556–568.
4. Ewen-Campen B, Donoughe S, Clarke DN, Extavour CG (2013) Germ cell specification requires zygotic mechanisms rather than germ plasm in a basally branching insect. *Curr Biol* 23(10):835–842.
5. Nieuwkoop PD (1951) Experimental observations on the origin and determination of the germ cells, and on the development of the lateral plates and germ ridges in the urodeles. *Arch Neerl Zool* 8(1):1–205.
6. Sutasurya LA, Nieuwkoop PD (1974) The induction of the primordial germ cells in the urodeles. *Wilhelm Roux' Archiv* 175(3):199–220.
7. Tam PP, Zhou SX (1996) The allocation of epiblast cells to ectodermal and germ-line lineages is influenced by the position of the cells in the gastrulating mouse embryo. *Dev Biol* 178(1):124–132.
8. Lawson KA, et al. (1999) *Bmp4* is required for the generation of primordial germ cells in the mouse embryo. *Genes Dev* 13(4):424–436.
9. Ying Y, Liu XM, Marble A, Lawson KA, Zhao GQ (2000) Requirement of *Bmp8b* for the generation of primordial germ cells in the mouse. *Mol Endocrinol* 14(7):1053–1063.
10. Ying Y, Zhao GQ (2001) Cooperation of endoderm-derived BMP2 and extraembryonic ectoderm-derived BMP4 in primordial germ cell generation in the mouse. *Dev Biol* 232(2):484–492.
11. Juliano CE, et al. (2006) Germ line determinants are not localized early in sea urchin development, but do accumulate in the small micromere lineage. *Dev Biol* 300(1): 406–415.
12. Brown FD, et al. (2009) Early lineage specification of long-lived germline precursors in the colonial ascidian *Botryllus schlosseri*. *Development* 136(20):3485–3494.
13. Kawamura K, et al. (2011) Germline cell formation and gonad regeneration in solitary and colonial ascidians. *Dev Dyn* 240(2):299–308.
14. Agee SJ, Lyons DC, Weisblat DA (2006) Maternal expression of a NANOS homolog is required for early development of the leech *Helobdella robusta*. *Dev Biol* 298(1):1–11.
15. Dearden PK (2006) Germ cell development in the Honeybee (Apis mellifera); vasa and nanos expression. *BMC Dev Biol* 6:6.
16. Dill KK, Seaver EC (2008) *Vasa* and *nanos* are coexpressed in somatic and germ line tissue from early embryonic cleavage stages through adulthood in the polychaete *Capitella sp. I*. *Dev Genes Evol* 218(9):453–463.
17. Bolker JA (1995) Model systems in developmental biology. *Bioessays* 17(5):451–455.
18. Ewen-Campen B, Srouji JR, Schwager EE, Extavour CG (2012) *Oskar* predates the evolution of germ plasm in insects. *Curr Biol* 22(23):2278–2283.
19. Hopf C, Viebahn C, Püschel B (2011) BMP signals and the transcriptional repressor BLIMP1 during germline segregation in the mammalian embryo. *Dev Genes Evol* 221(4):209–223.
20. de Sousa Lopes SMC, Hayashi K, Surani MA (2007) Proximal visceral endoderm and extraembryonic ectoderm regulate the formation of primordial germ cell precursors. *BMC Dev Biol* 7:140.
21. Niehrs C (2010) On growth and form: A Cartesian coordinate system of Wnt and BMP signaling specifies bilaterian body axes. *Development* 137(6):845–857.
22. Bollenbach T, et al. (2008) Precision of the Dpp gradient. *Development* 135(6): 1137–1146.
23. Piepenburg O, Grimmer D, Williams PH, Smith JC (2004) Activin redux: Specification of mesodermal pattern in *Xenopus* by graded concentrations of endogenous activin B. *Development* 131(20):4977–4986.
24. Chen Y, Schier AF (2001) The zebrafish Nodal signal Squint functions as a morphogen. *Nature* 411(6837):607–610.
25. Smith JC (1995) Mesoderm-inducing factors and mesodermal patterning. *Curr Opin Cell Biol* 7(6):856–861.
26. Frasch M (1995) Induction of visceral and cardiac mesoderm by ectodermal Dpp in the early *Drosophila* embryo. *Nature* 374(6521):464–467.
27. Staehling-Hampton K, Hoffmann FM, Baylies MK, Rushton E, Bate M (1994) *dpp* induces mesodermal gene expression in *Drosophila*. *Nature* 372(6508):783–786.
28. Wheeler WM (1893) A contribution to insect morphology. *J Morphol* 8(1):1–160.
29. Roonwal ML (1936) Studies on the embryology of the African migratory locust, *Locusta migratoria migratoides* R. and F. I. The early development, with a new theory of multi-phased gastrulation among insects. *Philos Trans R Soc Lond B Biol Sci* 226(538): 391–421.
30. Vrijens K, et al. (2013) Identification of small molecule activators of BMP signaling. *PLoS ONE* 8(3):e59045.
31. Hayashi K, et al. (2002) SMAD1 signaling is critical for initial commitment of germ cell lineage from mouse epiblast. *Mech Dev* 118(1-2):99–109.
32. Saitou M, Yamaji M (2012) Primordial germ cells in mice. *Cold Spring Harb Perspect Biol* 4(11):a008375.
33. Zeng V, et al. (2013) Gene discovery in a hemimetabolous insect: *De novo* annotation and assembly of a transcriptome for the cricket *Gryllus bimaculatus*. *PLoS ONE* 8(5): e61479.